J/ψ Production at CLAS12

R. Tyson

Vector Quarkonia as Pressure Gauges

27th of March 2026

J/ψ Near-Threshold Photoproduction

We are interested in measuring the process:

$$eN \rightarrow e'J/\psi N \rightarrow e'l^+l^-N$$

Close to the 8.2 GeV threshold, J/ψ photoproduction is predicted to be mediated by the exchange of two gluons.

The quark mechanical form factors can be probed with DVCS, TCS, DDVCS.

J/ψ allows to probe the gluonic mechanical form factors.

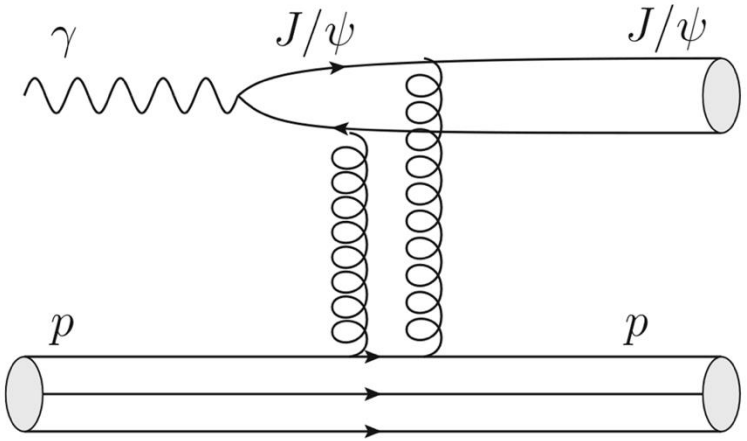

Pressure distribution of quarks inside the proton.

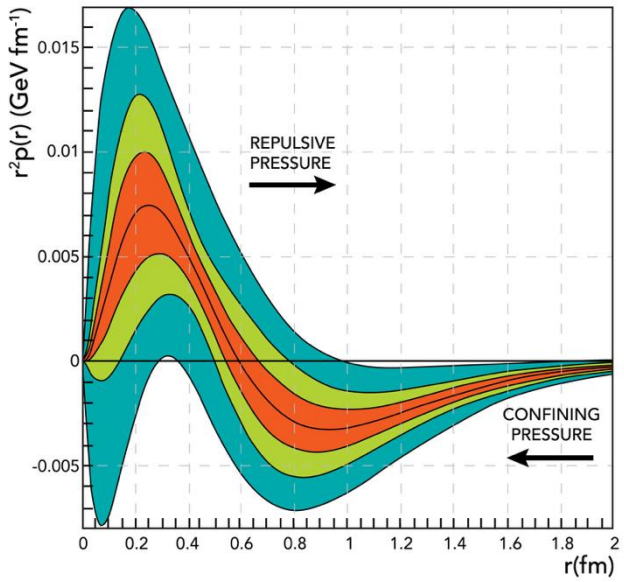

J/ψ Photoproduction on the Free Proton

GlueX – Hall D

The GlueX Collaboration has made measurements of the total and differential cross section over the full near-threshold range.

J/ψ 007 – Hall C

The J/ψ − 007 Collaboration has made measurements of the total and differential cross section as a function of t in 10 bins of E_γ in e^+e^- and $\mu^+\mu^-$ channels

CLAS12 – Hall B

The CLAS12 Collaboration has made measurements of the total and differential cross section as a function of t in e^+e^- channel

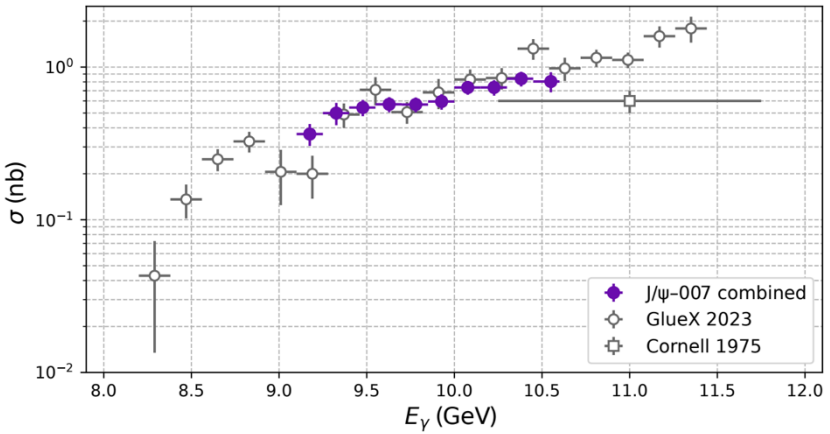

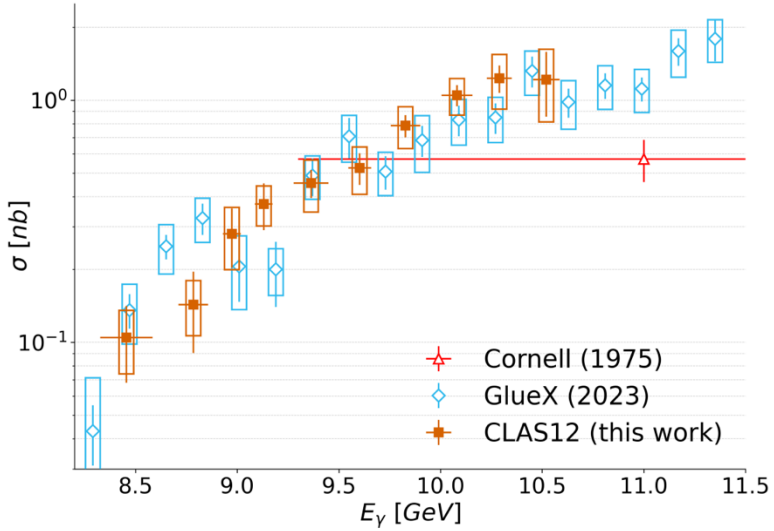

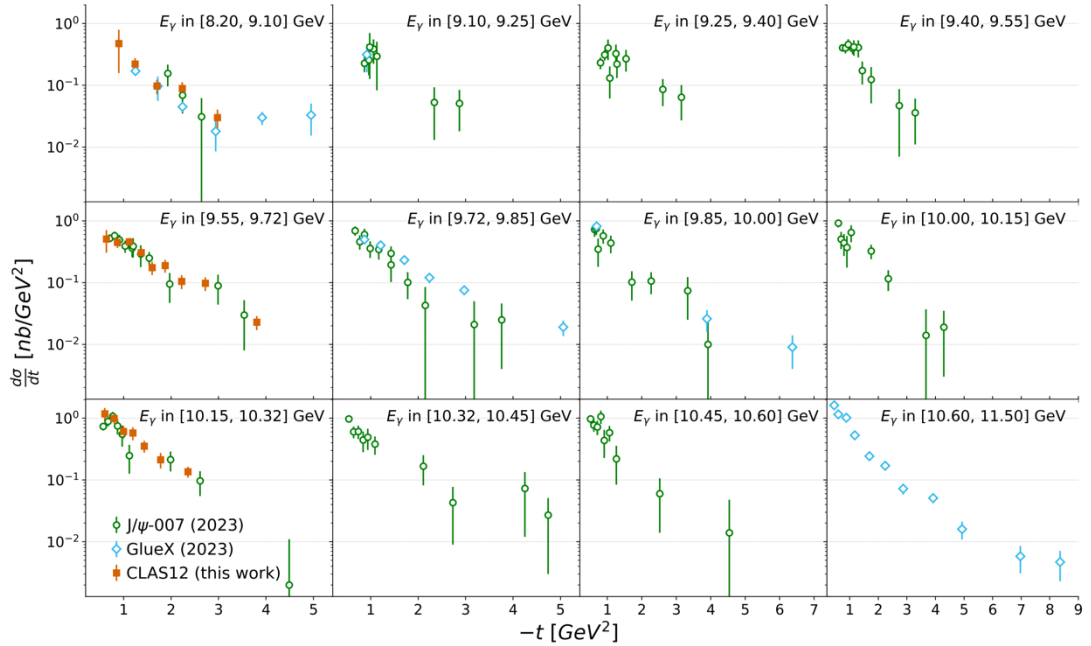

A. Ali, *et. al.* (GlueX Collaboration), *Phys. Rev. Lett.* **123,** 072001 (2019).
S. Adhikari *et al.* (GlueX Collaboration) *Phys. Rev. C* **108**, 025201 (2023).
D. Duran, et al. (J/ψ-007 Collaboration), *Nature* **615** (2023).
S. Joosten, et al. (J/ψ-007 Collaboration), arXiv:2602.14416 (2026).
P. Chatagnon, et al. (CLAS Collaboration) arXiv:2602.22128 (2026).

Holographic QCD & GPDs

In holographic QCD a higher dimensional duality relates spin-2 fields to gravity. J/ψ is produced by the exchange of gravitons (tensor 2++glueballs) and scalar (0++) glueballs.

In the GPD framework, large skewness at threshold allows to relate the scattering amplitude to gluon GPDs. The GFFs are extracted from the first moments of the GPDs .

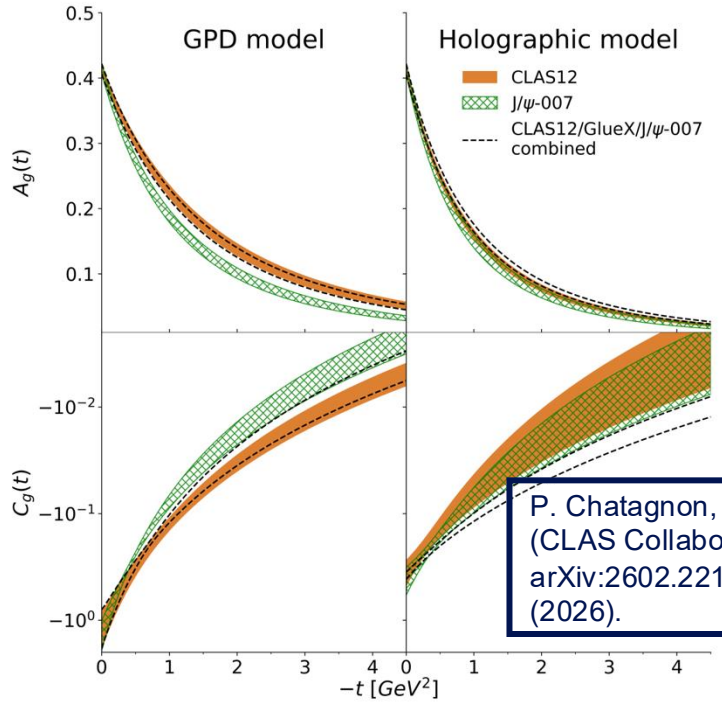

P. Chatagnon, et al. (CLAS Collaboration) arXiv:2602.22128 (2026).

Gluonic pressure distribution in the Breit frame in GeV/fm from J/ψ – 007 data

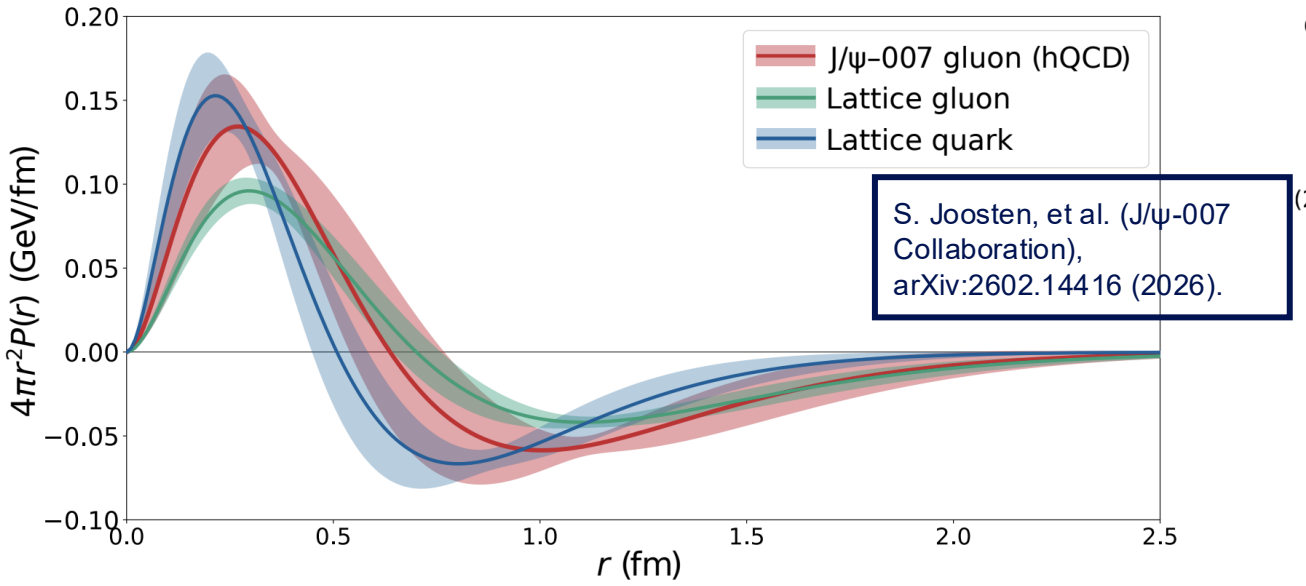

S. Joosten, et al. (J/ψ-007 Collaboration), arXiv:2602.14416 (2026).

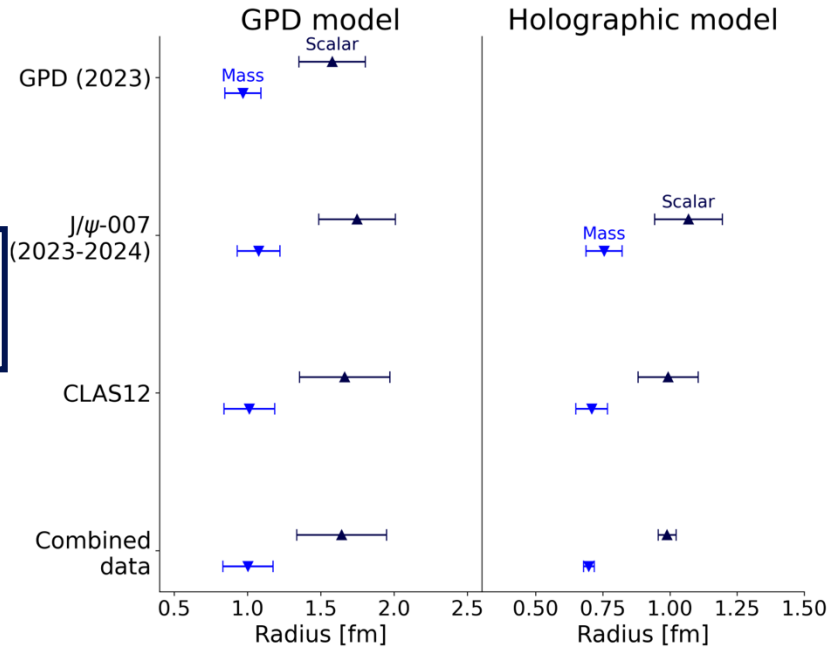

Production Mechanism

Several different proposed near-threshold production mechanisms:

- Two-gluon exchange
- Higher (lower) twist 3 (1) gluon exchange
- Open-Charm intermediate states
- Pomeron exchange
- Meson exchange
- 2015, 2019 LHCb pentaquarks

Need higher statistical precision and polarization observables to distinguish between production mechanisms.

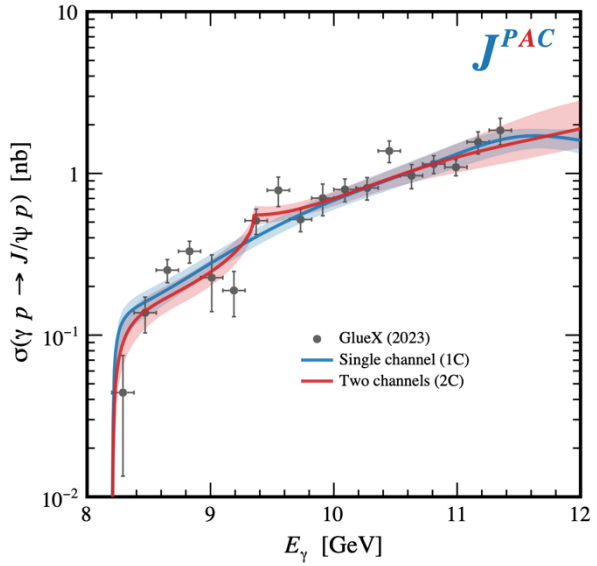

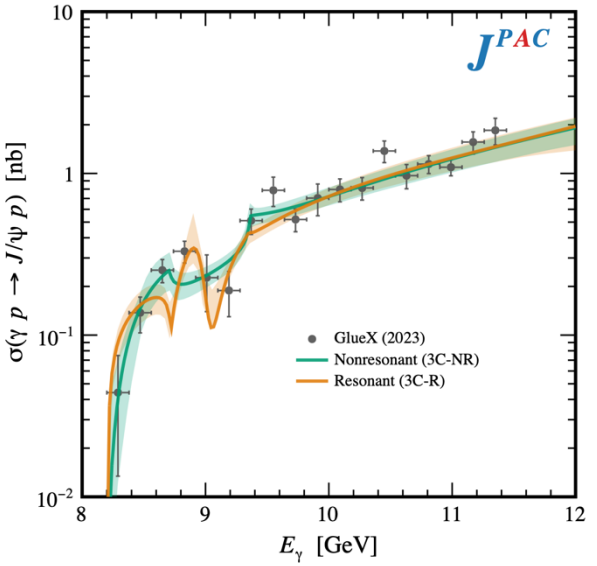

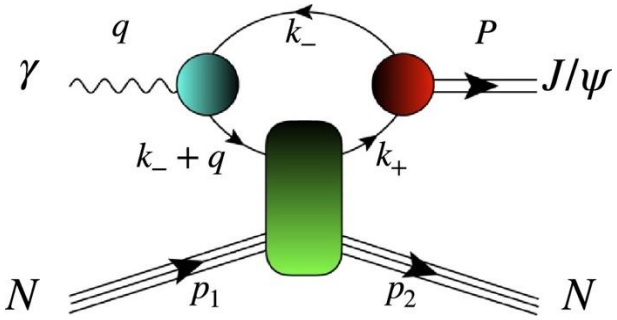

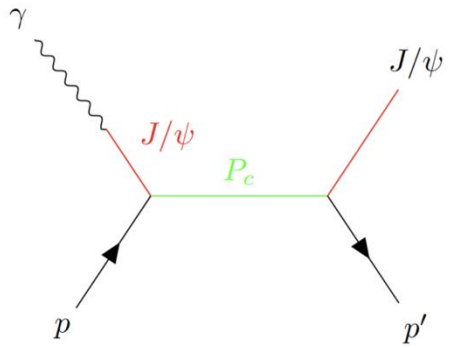

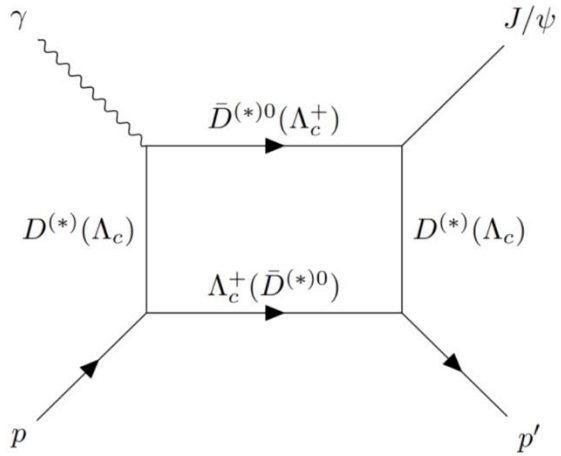

M.-L. Du, *et. al., Eur. Phys. J. C* **80** 1053 (2020).
D. Winney, *et. al.* (Joint Physics Analysis Center), *Phys. Rev. D* **108** 054018 (2023).
L.Tang, Y.-X. Yang, Z.-F. Cui, C. D. Roberts, *Phys. Lett. B* **856** 138904 (2024).
S.H. Kim, *Phys. Lett. B,* **868** 139725 (2025).
S.J. Brodsky, E. Chudakov, P. Hoyer, J.M. Laget, *Phys.Lett. B* **498** 23 (2001).

J/ψ Production and Nuclear Structure

Comparing J/ψ production on bound vs free proton could hint towards modification of gluon structure of the nucleon in nuclei.

Can also think of coherent production on the deuteron (nuclei?).

It's been argued that subthreshold production can be a probe of nuclear and SRC structure.

First measurements from SRC-CT (Hall D) contain possible hints of increased subthreshold cross section. Point to:

- Increased gluon density
- Decreased gluon radius

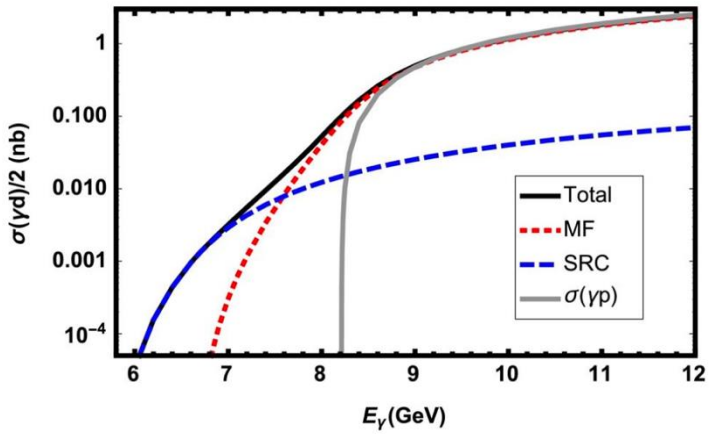

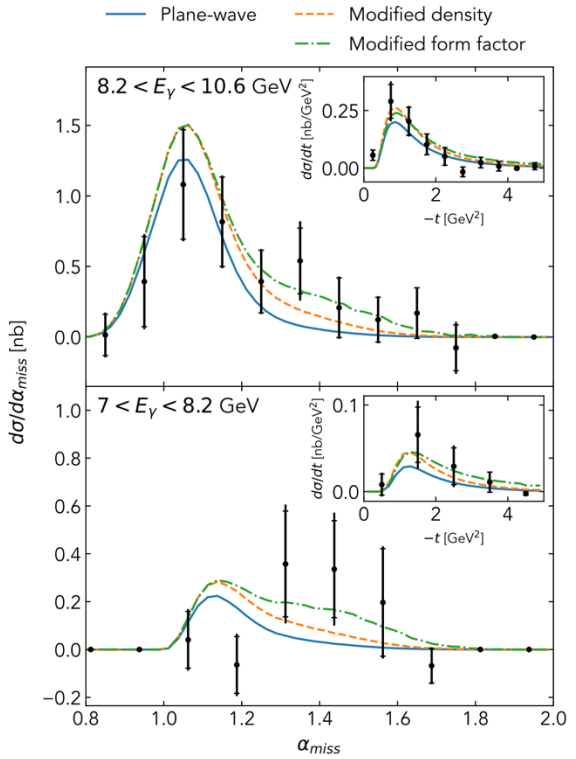

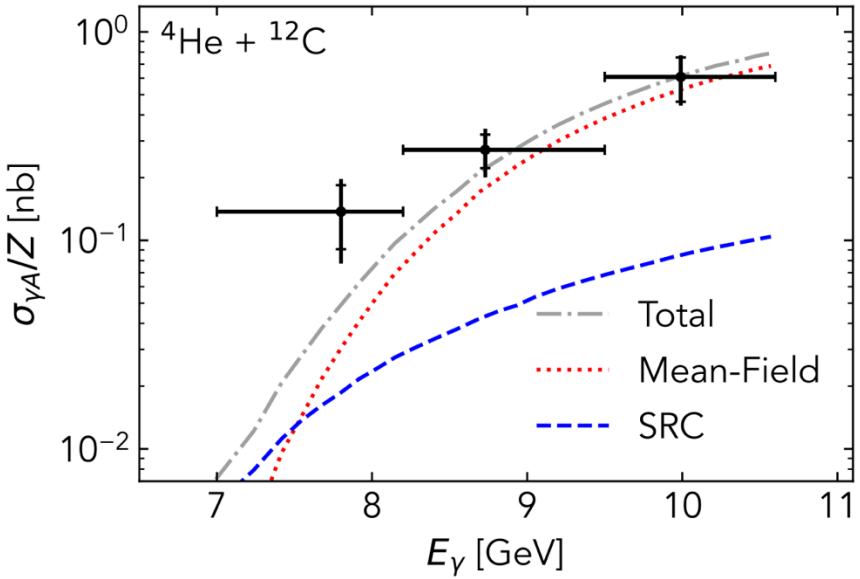

Y. Hatta, et al., *Phys. Lett. B,* **803**, 10 35321 (2020).
J. R. Pybus, et al. (SRC-CT Collaboration) *Phys Rev Lett* **134**, 201903 (2025)

What More Can CLAS12 Offer?

CLAS12 has taken several datasets relevant to the points addressed in previous slides.

The RG-B experiment employed a deuterium target.

The RG-C experiment employed a longitudinally polarized NH3 target

The RG-D and RG-E experiments employed a range of nuclear targets (D2, C, Al, Cu, Sn, Pb)

We can look at various channels:

$$ep \rightarrow e'J/\psi\, p \rightarrow (e')e^+e^-p \quad \text{(free proton)}$$
$$e\, p_{bound} \rightarrow e'J/\psi\, p \rightarrow (e')e^+e^-p \quad \text{(incoherent)}$$
$$e\, n_{bound} \rightarrow e'J/\psi\, n \rightarrow (e')e^+e^-n \quad \text{(incoherent)}$$
$$ed \rightarrow e'J/\psi\, d \rightarrow (e')e^+e^-d \quad \text{(coherent on d)}$$

RG-D

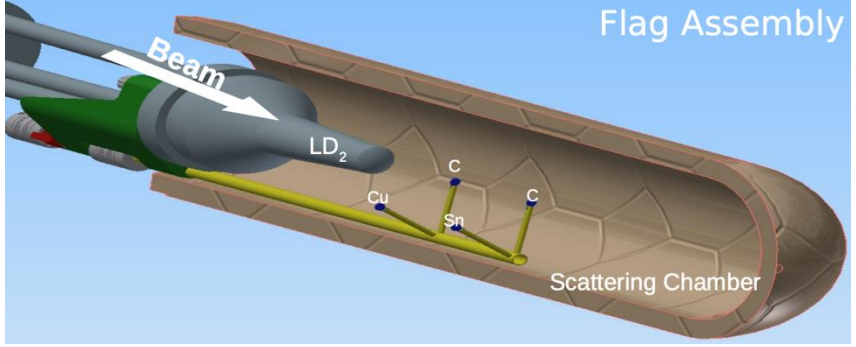

RG-E

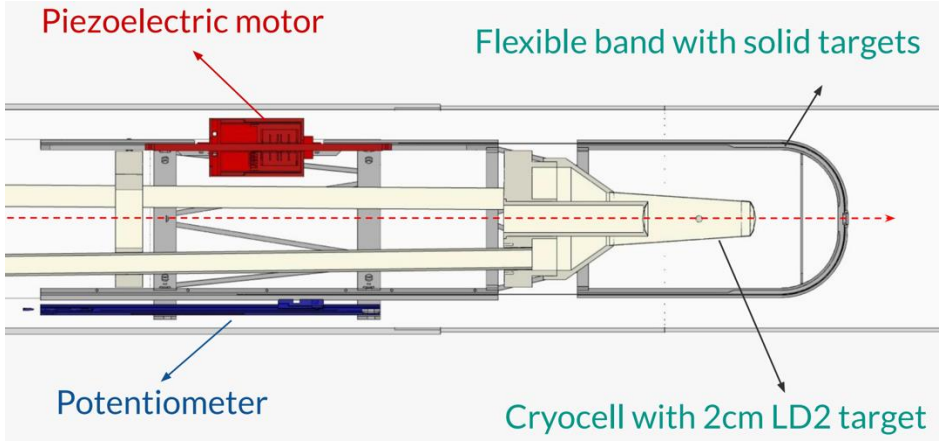

Experiment	Target(s)	Accumulated Charge (mC)	Data Status
RG-A	LH2	114 mC	Available
RG-B	LD2	107 mC	Available
RG-C	NH3 (long. pol.)	13 mC	Available
RG-D	LD2, CuSn, CxC	32, 183, 33 mC	In postprocessing
RG-E	LD2+ C, LD2+Al, LD2+Cu, LD2+Sn, LD2+Pb,	24, 21, 22, 22, 27 mC	Ready for postprocessing

University of Glasgow

CLAS12

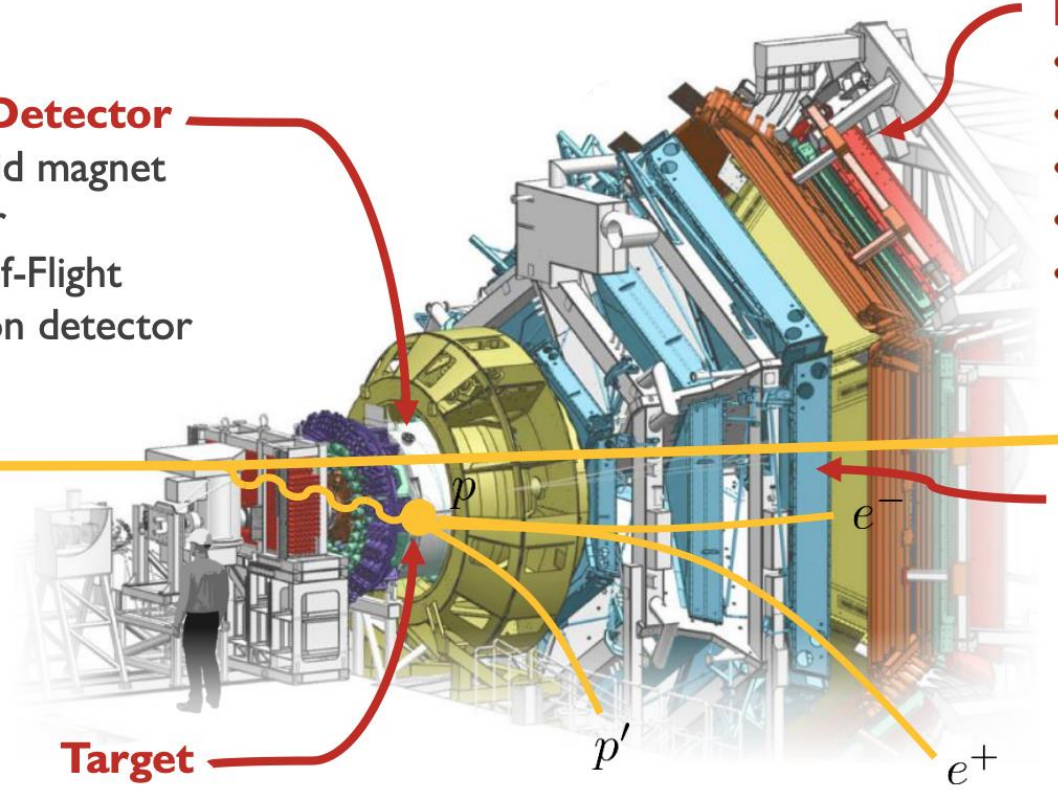

Central Detector
- Solenoid magnet
- Tracker
- Time-of-Flight
- Neutron detector

Forward Detector
- Torus magnet
- Drift Chambers
- Time-of-Flight
- Calorimeters
- Cherenkov counters

Beam
- 85% longitudinally polarized e^-
- Max. luminosity: 10^{35} $s^{-1}cm^{-2}$
- Energy up to ~10.6 GeV

Forward Tagger
- Calorimeter
- Time-of-Flight
- Tracker

Target
- **Proton**
- **Deuterium**
- Longitudinally pol. H/D
- Nuclear targets

Cross Section Calculation

Total cross section as a function of quasi-real virtual photon energy

Number of J/ψ from fit in E_γ bins

$$\sigma_0(E_\gamma) = \frac{N_{J/\psi}(E_\gamma)}{N_\gamma(E_\gamma) \cdot l_T \cdot \rho_T \cdot Br \cdot R_c(E_\gamma) \cdot \epsilon(E_\gamma) \cdot \omega_c}$$

Luminosity:
N_γ is calculated from the photon flux
l_T and ρ_T are the target length and density

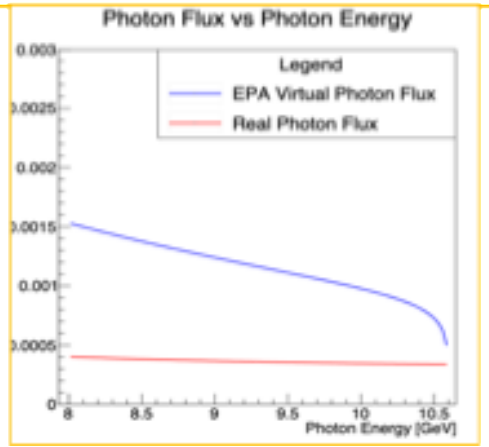

6 % Branching Ratio ($J/\psi \rightarrow e^+e^-$)

Efficiency in E_γ bins from MC

Radiative Corrections

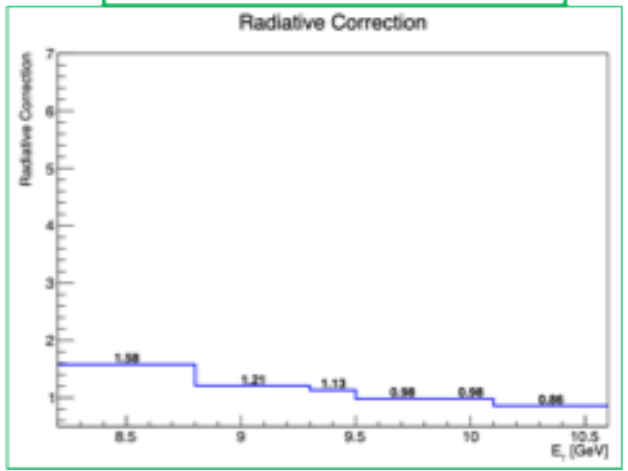

Normalisation to Bethe Heitler process

Could also call this a correction to the efficiency and flux calculations.

Efficiency & Normalisation

P. Chatagnon, et al. (CLAS Collaboration) arXiv:2602.22128 (2026).

The efficiency calculation takes into account geometrical acceptance and detection efficiency effects on the measured J/ψ rate, generally obtained from MC.

Several corrections are applied to the MC:

- Smearing to reconstructed momentum and angles.
- Neutron detection efficiency.
- Reconstruction efficiency as a function of beam current.
- Efficiency ratios for e+/e- PID and exclusivity cuts.

Further compare the expected number of Bethe Heitler events in MC to that in CLAS12 data in the invariant mass region of 2.0 - 2.9 GeV. This accounts for errors in the efficiency and flux calculations.

Systematic uncertainty on the Bethe Heitler normalization 10 - 20 %.

Necessary (if not, very helpful) for analyses, needs accurate Bethe Heitler modelling for various targets.

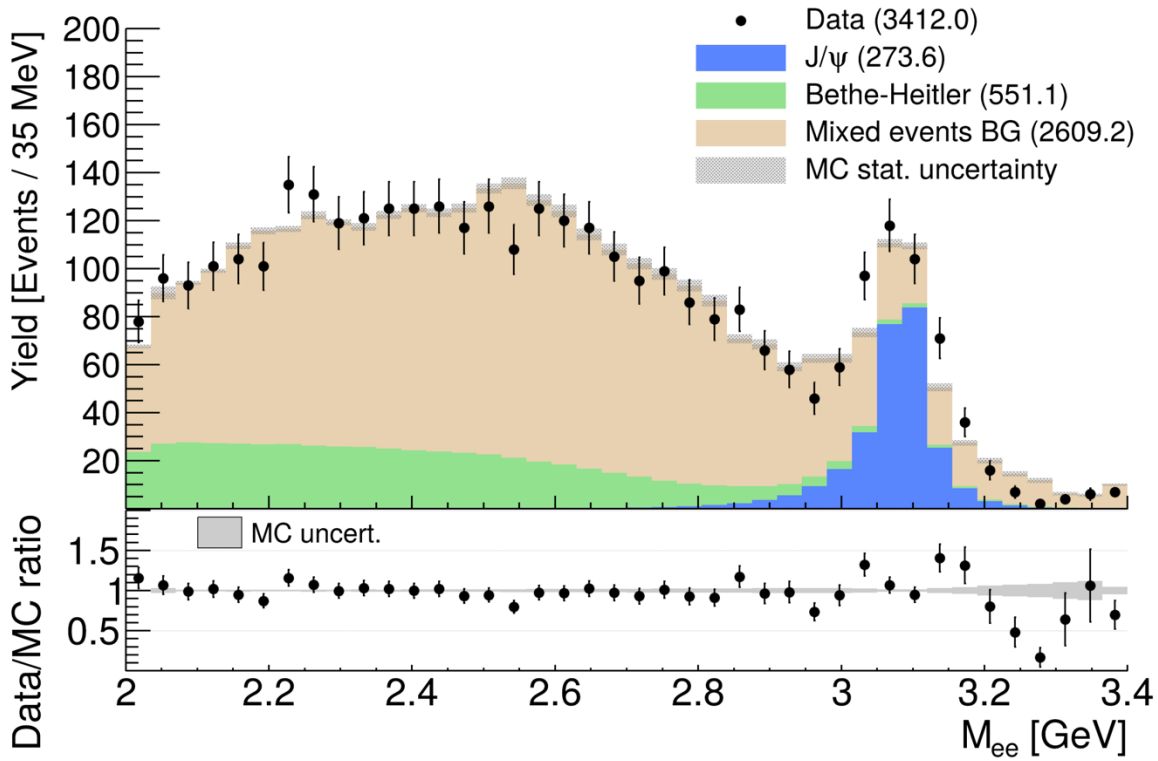

Incoherent J/ψ Production in LD2

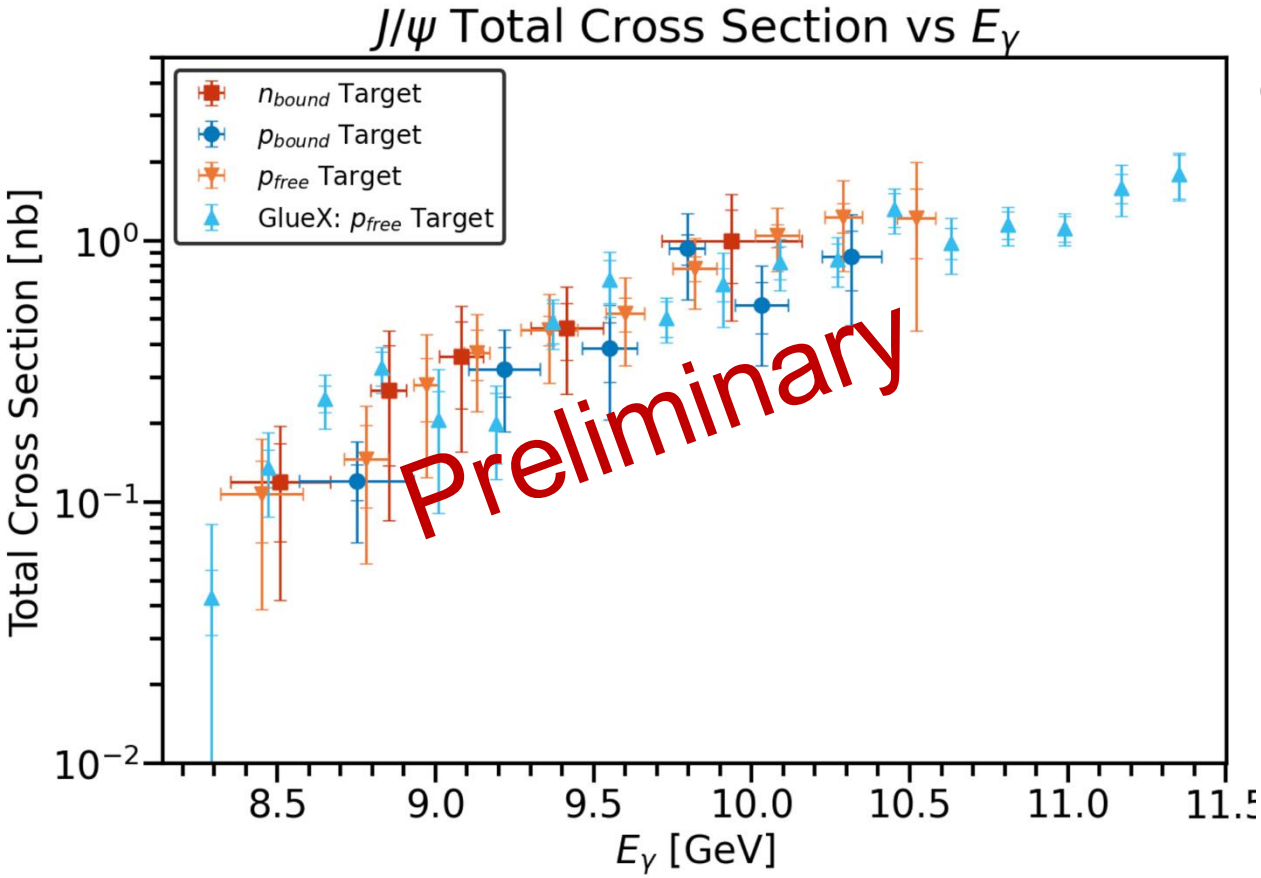

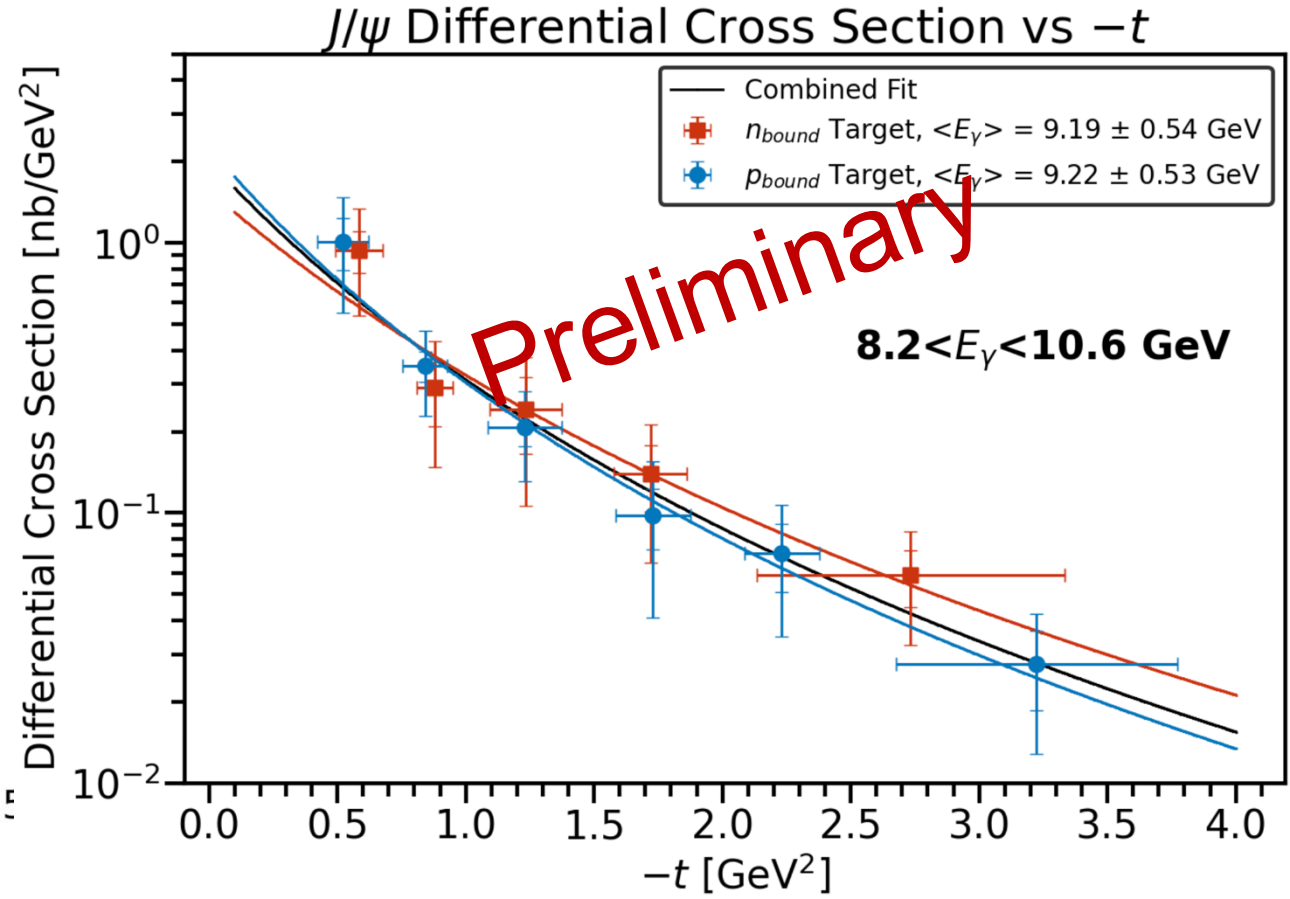

Analysis Note in CLAS Collaboration review

Incoherent J/ψ Production in LD2

Fit the mechanical form factors shown below to differential cross section:

$$< N'|T^{\mu,\nu}_{q,g}|N >= \bar{u}(N')\left(A_{q,g}(t)\gamma^{\mu p\nu} + B_{q,g}(t)\frac{iP^{\mu\sigma\nu}\rho\Delta_\rho}{2M} + C_{q,g}(t)\frac{\Delta^\mu\Delta^\nu - g^{\mu\nu}\Delta^2}{M} + \bar{C}_{q,g}(t)Mg^{\mu\nu}\right)u(N)$$

Some assumptions in fit:

- Assume dominant two-gluon production mechanism
- Assume FSI contribution to cross section much smaller than plane wave impulse approximation (A. Freese, M.M Sargsian, *Phys. Rev. C* **88**, 044604 (2013.))
- Neglect $B(t)$ and $\bar{C}(t)$.
- Assume tripole shape for mechanical form factors:

$$A_g(t) = \frac{A_g(0)}{\left(1-\frac{t}{m_A}\right)^3}, C_g(t) = \frac{C_g(0)}{\left(1-\frac{t}{m_A}\right)^3}$$

- Gaussian constrained with $A_{t=0}$ constrained to the average gluon PDF from CT18, m_C to free proton data.

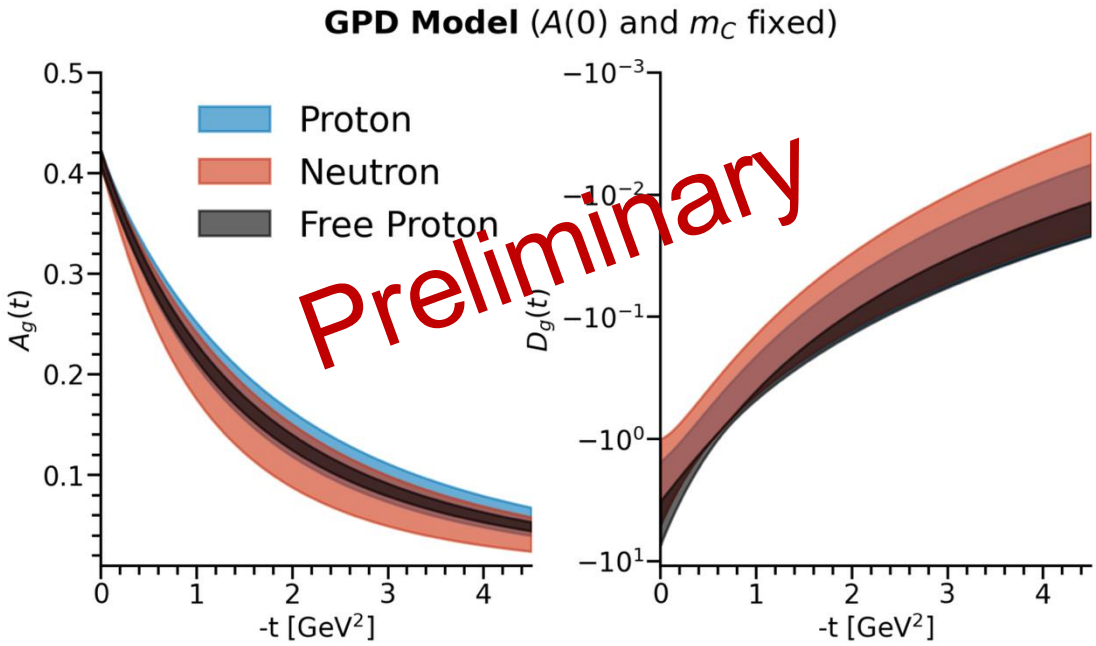

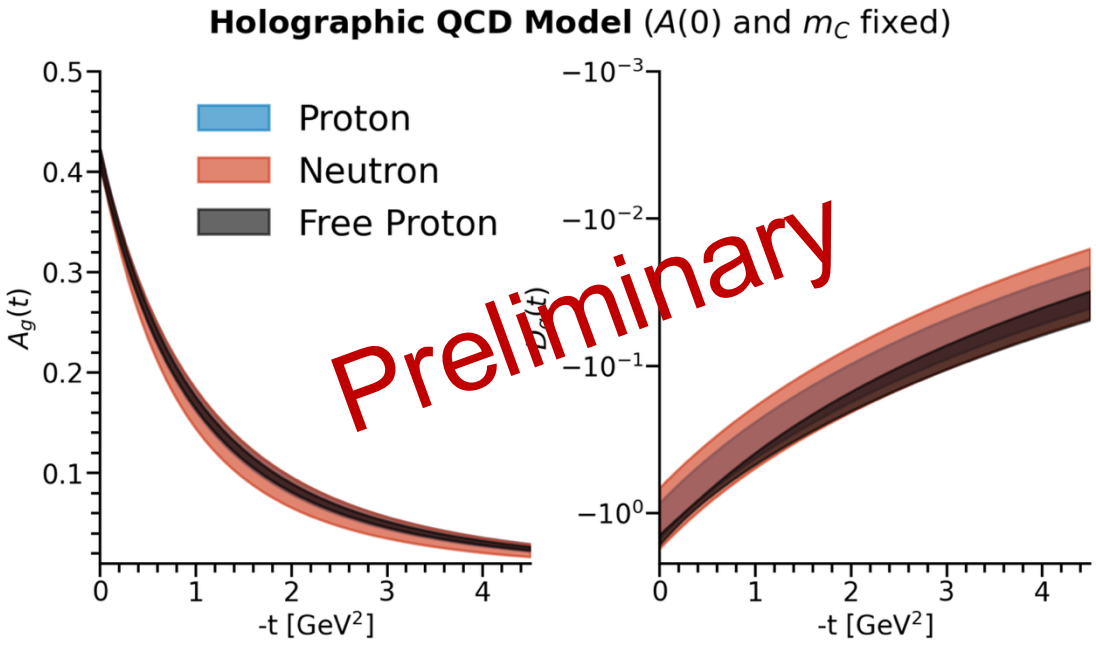

Incoherent J/ψ Production in LD2

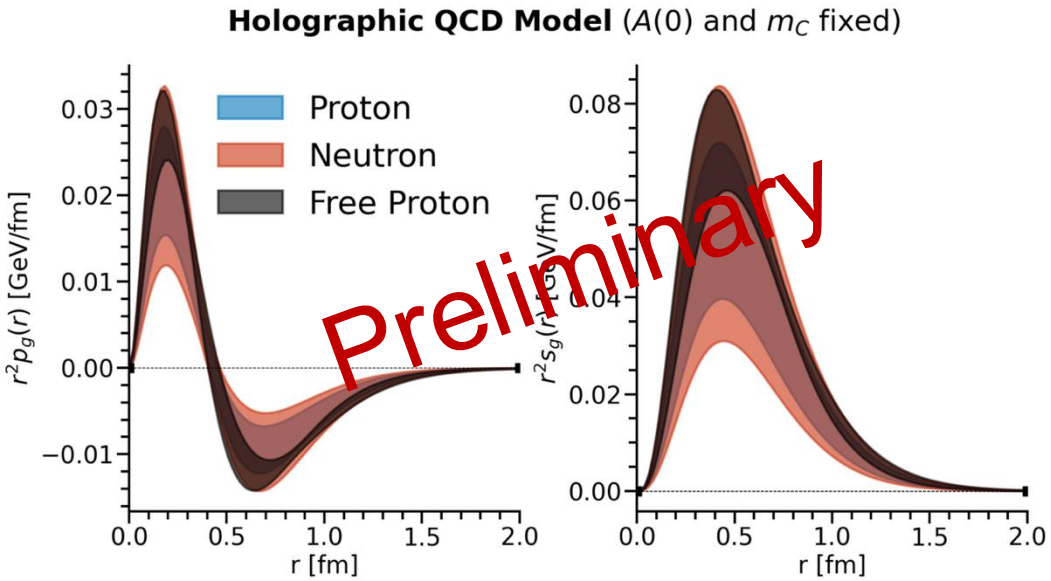

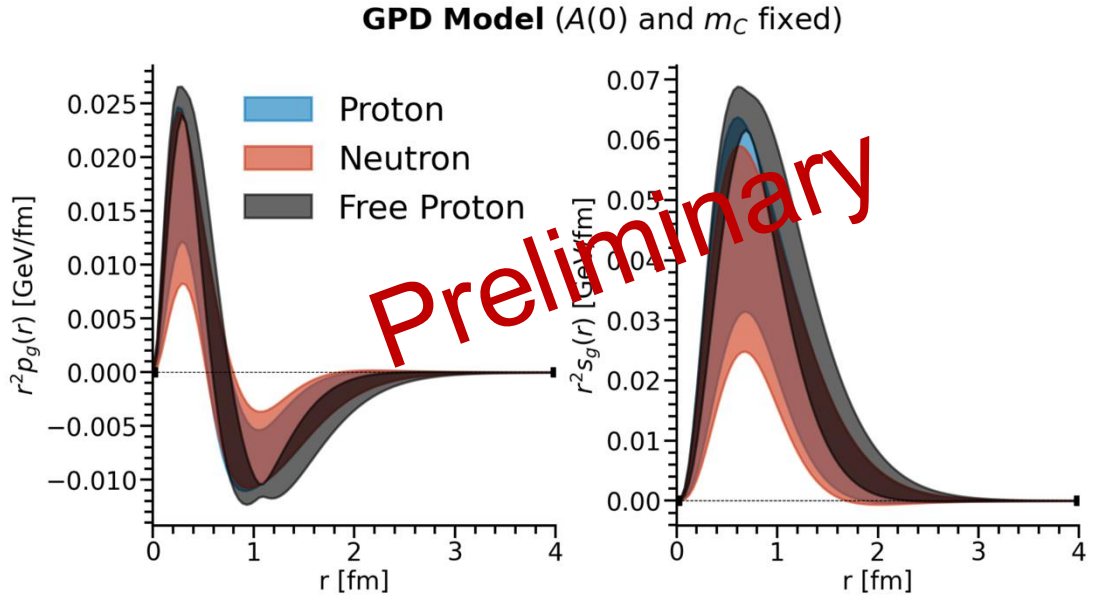

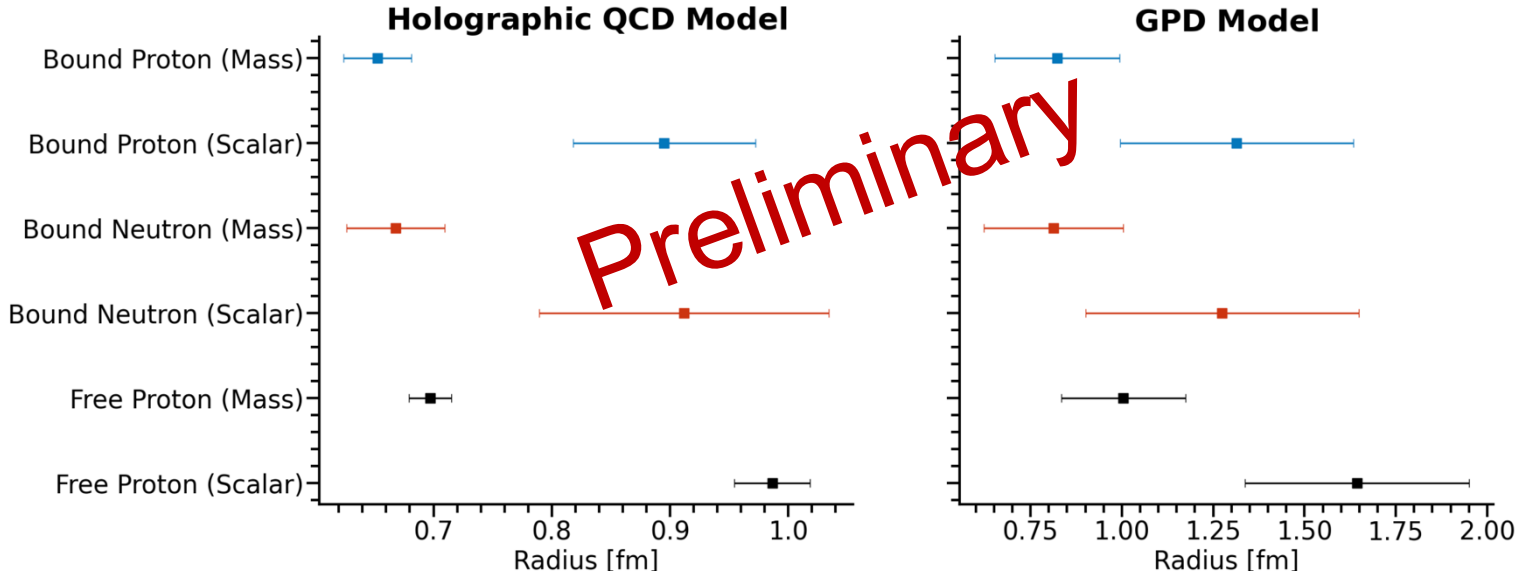

J/ψ Polarisation Observables

D.Winney, et al. (JPAC Collaboration), *Phys. Rev. D* **100**, 034019 (2019).

Predictions from JPAC on Double Spin Asymmetry for LHCb pentaquark production.

Possible further predictions for open-charm and gluon exchange production mechanism.

Aim is to measure:

- Unpolarised Spin Density Matrix Elements (SDMEs)
- Beam Spin Asymmetry (BSA)
- Target Spin Asymmetry
- Double Spin Asymmetry

Compare BSA and SDME measurements on longitudinally polarised and unpolarised targets.

Aim to submit CLAS Approved Analysis note (K. Gates) in coming months (internal CLAS proposal system).

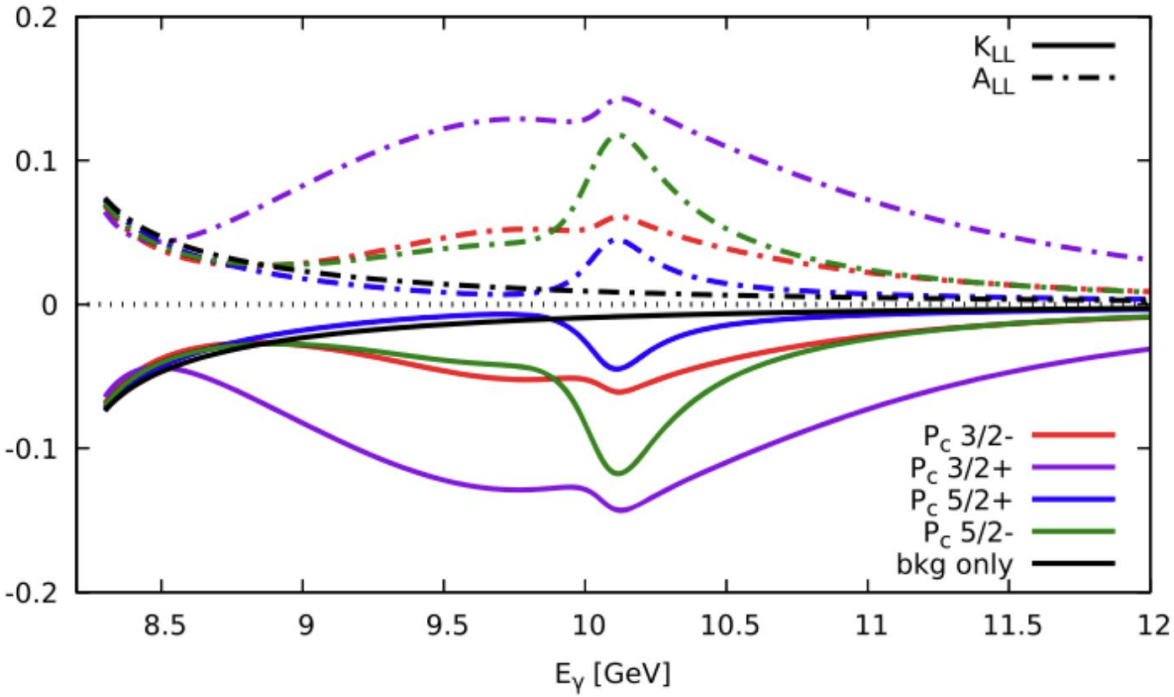

BSA; $$A_{LU} = \frac{P_t^-(N^{++} - N^{-+}) + P_t^+(N^{+-} - N^{--})}{Pb \times (P_t^-(N^{++} + N^{-+}) + P_t^+(N^{+-} + N^{--}))}$$

TSA; $$A_{UL} = \frac{N^{++} + N^{-+} - N^{+-} - N^{--}}{Df \times (P_t^-(N^{++} + N^{-+}) + P_t^+(N^{+-} + N^{--}))}$$

DSA; $$A_{LL} = \frac{N^{++} + N^{--} - N^{+-} - N^{-+}}{P_B \cdot D_f(P_T^-(N^{++} + N^{-+}) + P_T^+(N^{+-} + N^{--}))}$$

J/ψ Polarisation Observables

K. Gates

Predictions from JPAC on Double Spin Asymmetry for LHCb pentaquark production.

Possible further predictions for open-charm and gluon exchange production mechanism.

Aim is to measure:

- Unpolarised Spin Density Matrix Elements (SDMEs)
- Beam Spin Asymmetry (BSA)
- Target Spin Asymmetry
- Double Spin Asymmetry

Compare BSA and SDME measurements on longitudinally polarised and unpolarised targets.

Aim to submit CLAS Approved Analysis note (K. Gates) in coming months (internal CLAS proposal system).

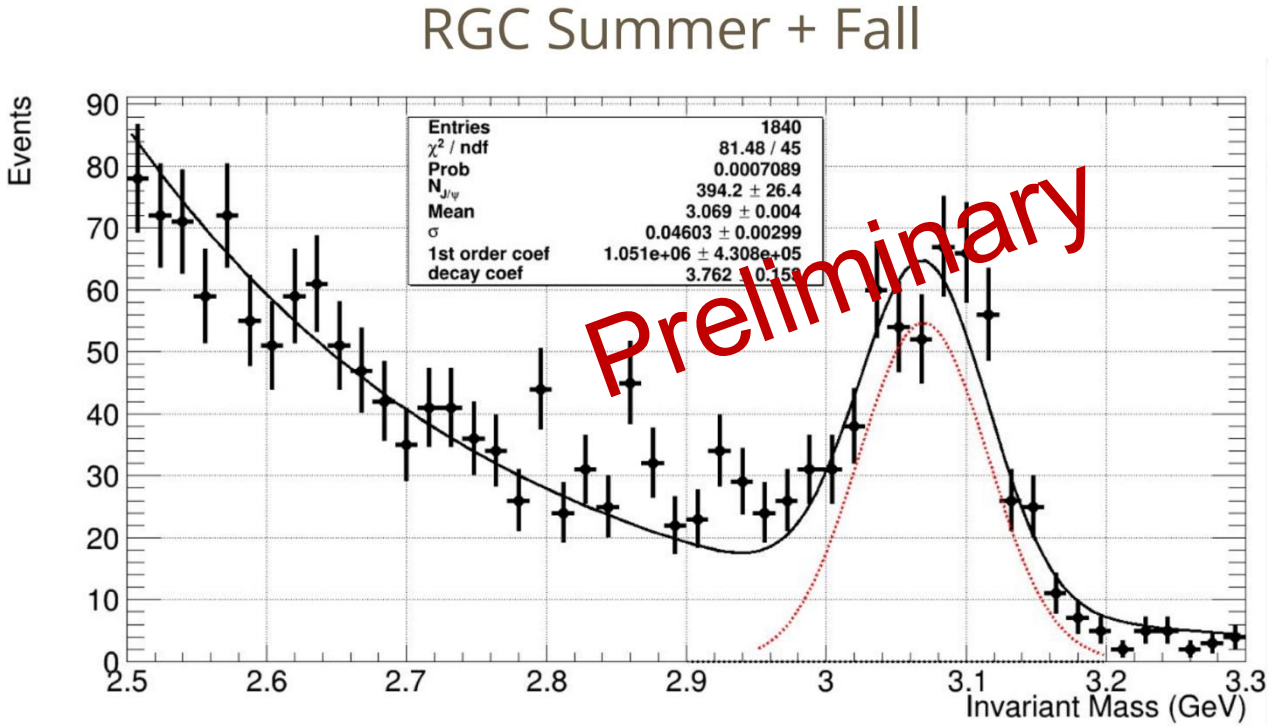

BSA; $$A_{LU} = \frac{P_t^-(N^{++} - N^{-+}) + P_t^+(N^{+-} - N^{--})}{Pb \times (P_t^-(N^{++} + N^{-+}) + P_t^+(N^{+-} + N^{--}))}$$

TSA; $$A_{UL} = \frac{N^{++} + N^{-+} - N^{+-} - N^{--}}{Df \times (P_t^-(N^{++} + N^{-+}) + P_t^+(N^{+-} + N^{--}))}$$

DSA; $$A_{LL} = \frac{N^{++} + N^{--} - N^{+-} - N^{-+}}{P_B \cdot D_f(P_T^-(N^{++} + N^{-+}) + P_T^+(N^{+-} + N^{--}))}$$

Incoherent J/ψ Yield Estimation with Nuclear Targets

P. Chatagnon

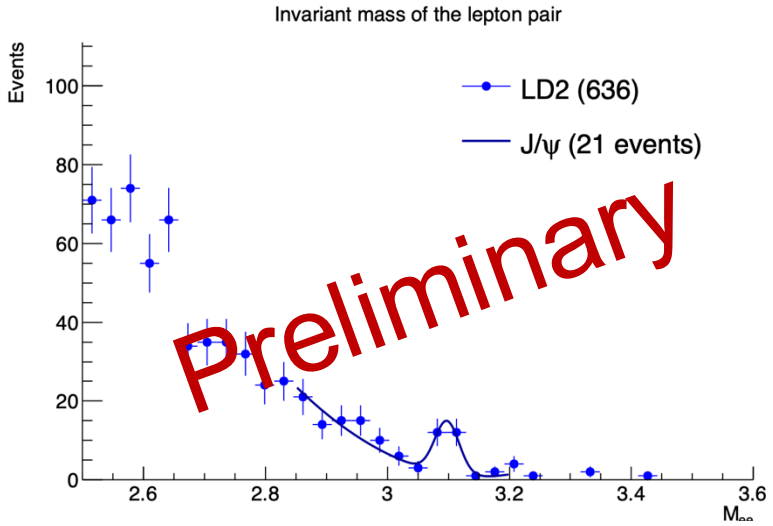

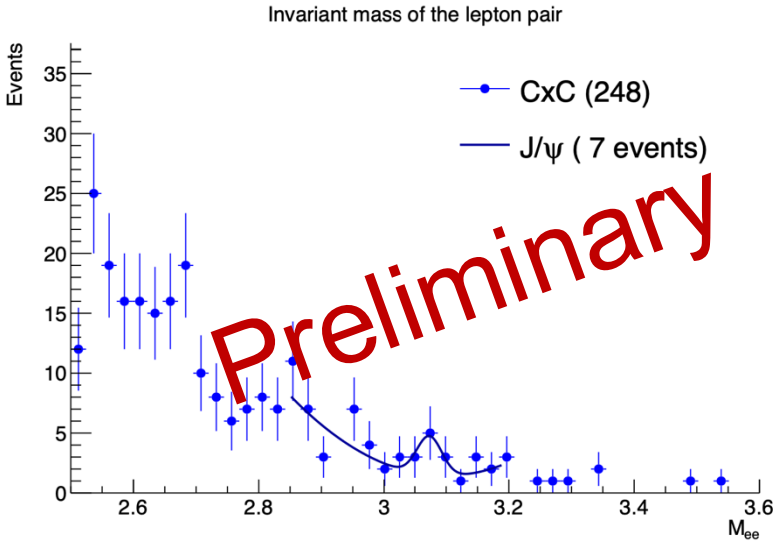

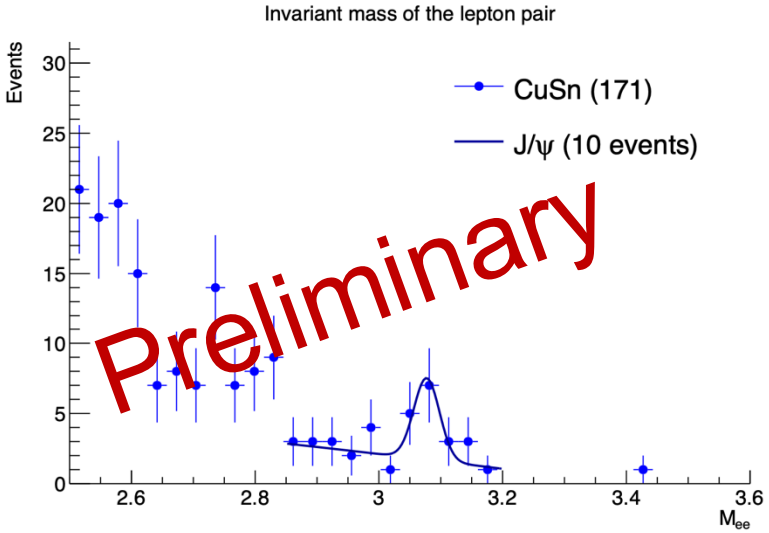

Expected final yields on full RG-D dataset

LD2: ~210

CxC: ~70

Cu/Sn: ~100

Yield estimation with ~10% of RG-D (P. Chatagnon), full dataset is currently being processed.

Two datasets RG-D, and RG-E.

RG-E will have better acceptance due to torus magnet polarity ⟹ more than double statistics.

GlueX published measurements:

- ~50 J/ψ on C
- ~45 J/ψ on He
- ~25 J/ψ on D

Incoherent ϕ Yield Estimation with Nuclear Targets

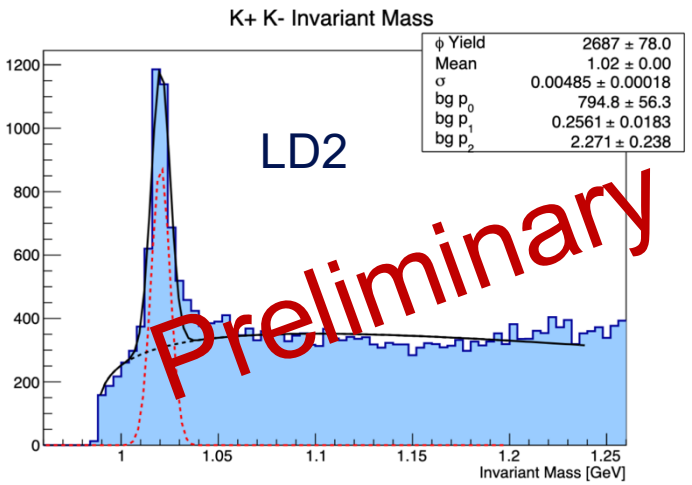

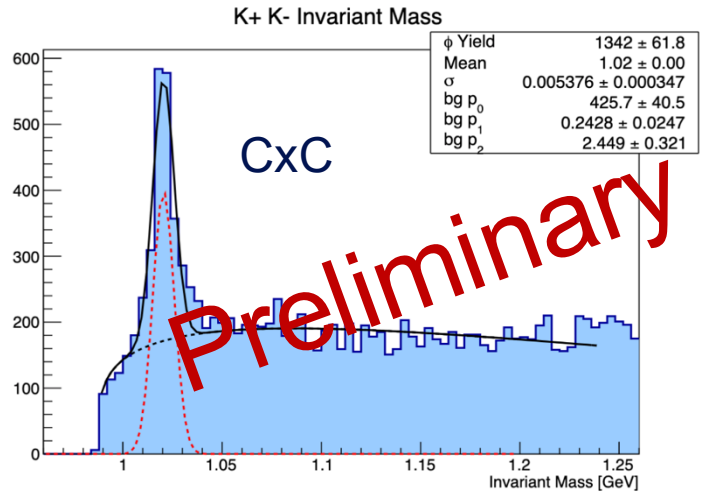

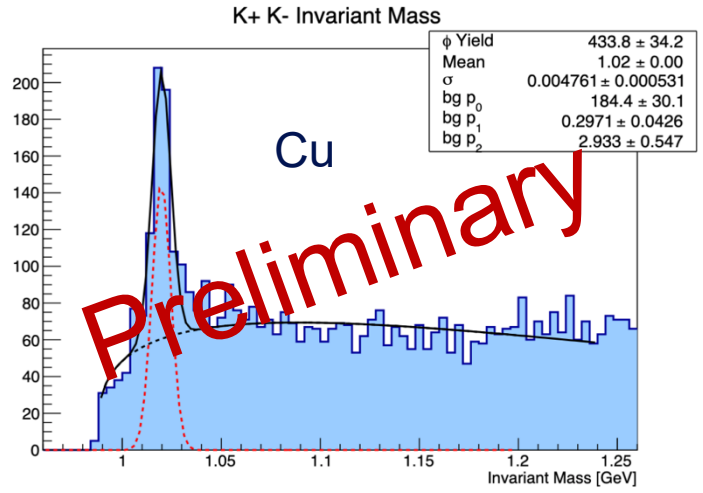

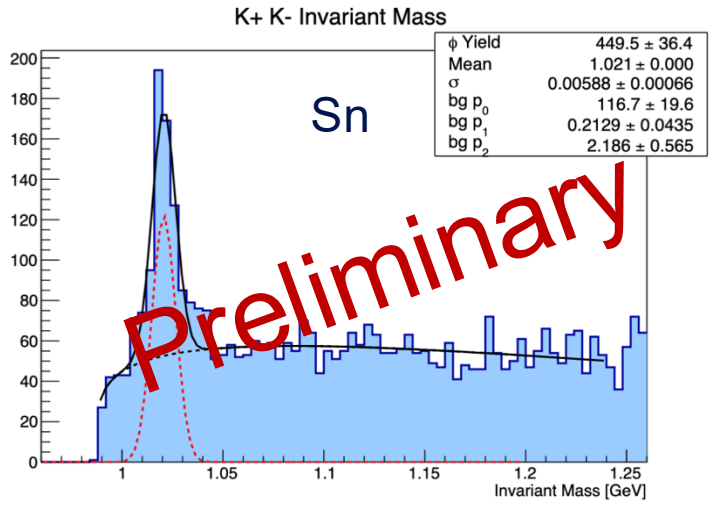

Two datasets RG-D, and RG-E, yield estimation with ~10% of RG-D.

Expected final yields on full RG-D dataset

- LD2: ~ 25000
- CxC: ~13000
- Cu: ~ 4500
- Sn: ~ 4500

Aim to probe:

- Cross section ratios (function of x)
- Q^2 dependence
- Model dependent FSI contribution
- Coherent production on d (Q^2 dependence)
- Coherent production via entanglement enabled intensity interferometry?

More Data

RG-A (LH2 target) and RG-B (LD2 target) have ~half of data left to take. Upgrades to reconstruction software and planned detector upgrades should allow to run at higher beam currents.

RG-C (polarized NH3) has 40 PAC days remaining (tentatively scheduled for FY28).

Yield estimates from RG-D (nuclear targets) used 10% of data. RG-E (nuclear targets) will more than double statistics for J/ψ.

RG-D and RG-E both employed LD2 targets, can be used to improve incoherent J/ψ on bound nucleon and coherent J/ψ on deuteron statistics.

We could investigate J/ψ decay to $\mu^+\mu^-$ in RG-A/RG-B/RG-C.

μCLAS12 will be provide high statistics for J/ψ on LH2. μCLAS12 with LD2?

Conclusion

CLAS12 has released measurements of the total and differential cross section on the free proton.

Plenty more interesting results to come:

- Measurements on the bound proton and neutron in deuterium (analysis note in collaboration review)
- Measurements of polarization observables, including on longitudinally polarized targets (early stage, going to get CAA approval)
- Measurements on nuclear targets (CAA approved)

Few things I didn't have time to discuss further:

- Coherent production on deuteron (N. Silva, Y. Ilieva)
- Coherent production via entanglement enabled intensity interferometry in nuclear targets?

Theory support and suggestions always welcome!!

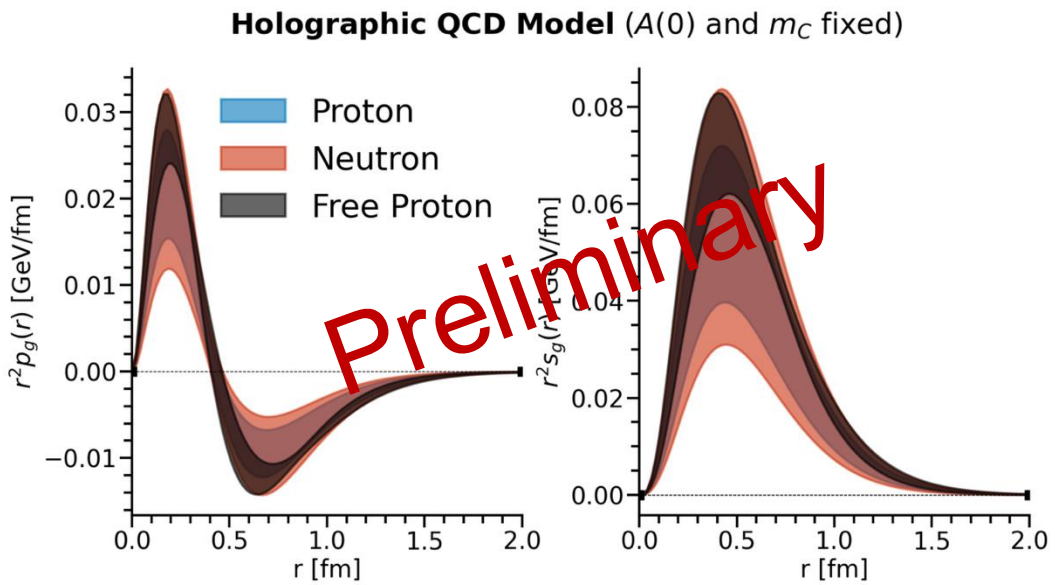

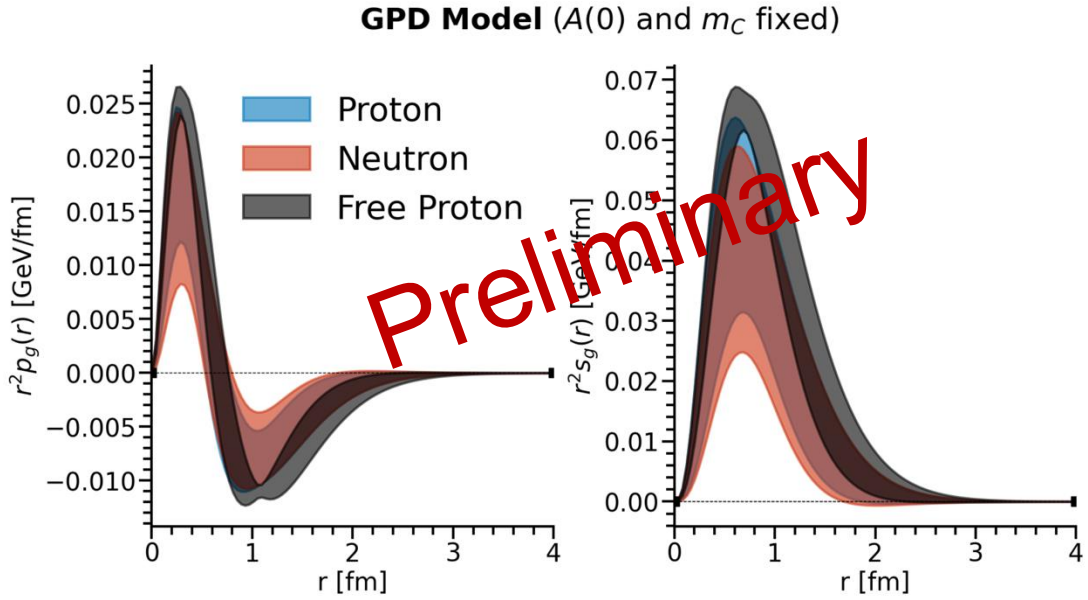

Back-up Slides

General Analysis Steps

P. Chatagnon, et al. (CLAS Collaboration) arXiv:2602.22128 (2026).

Particle & Event Selection

Momentum measured by drift chambers.

Time of Flight Detectors used for hadron PID.

High Threshold Cherenkov Counters and electromagnetic calorimeters used to ID electrons,

Above 4.5 GeV, employ ML based PID.

Use cuts on Q^2 and missing mass squared from:

$$eN \rightarrow e^+e^-N(X)$$

-t measured using recoil nucleon. E_γ measured from final state e^+e^-N

Yield obtained by fitting e^+e^- invariant mass.

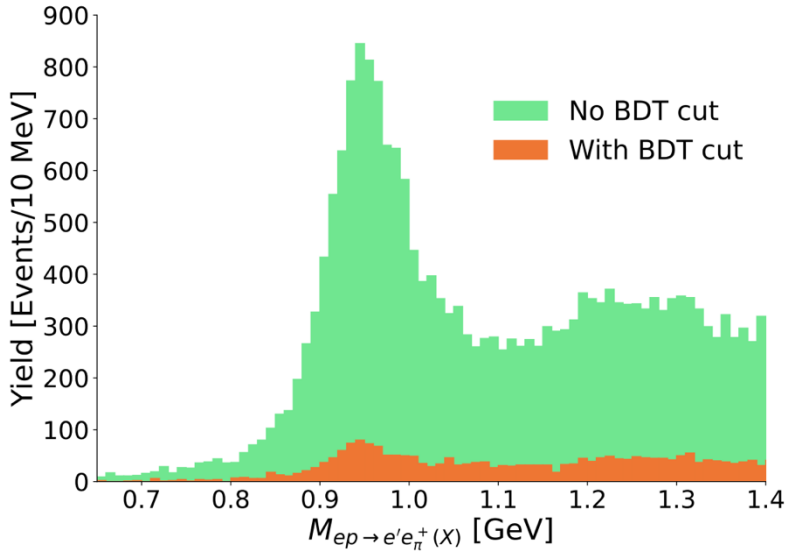

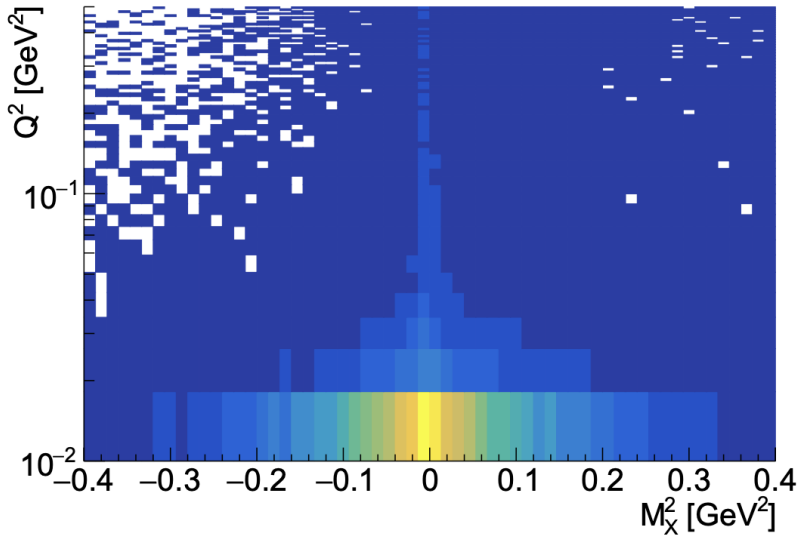

Suppressing π^+ IDed as e^+.

Vector Meson Dominance Framework

P. Chatagnon, et al. (CLAS Collaboration) arXiv:2602.22128 (2026).

The nucleon mass can be decomposed into the contributions from the quark masses, the energy of quarks and gluons and the trace anomaly contribution .

A scalar gravitational form factor $G(t)$ gives access to the mass radius of the nucleon. Assuming a dipole form for $G(t)$:

$$\frac{d\sigma}{dt} = G(t)^2 = \left(\frac{M_p}{(1-\frac{t}{m_s^2})^2}\right)^2$$

The mass radius r_m is calculated from the free parameter m_s:

$$r_m = \frac{\sqrt{12}\hbar c}{m_s}$$

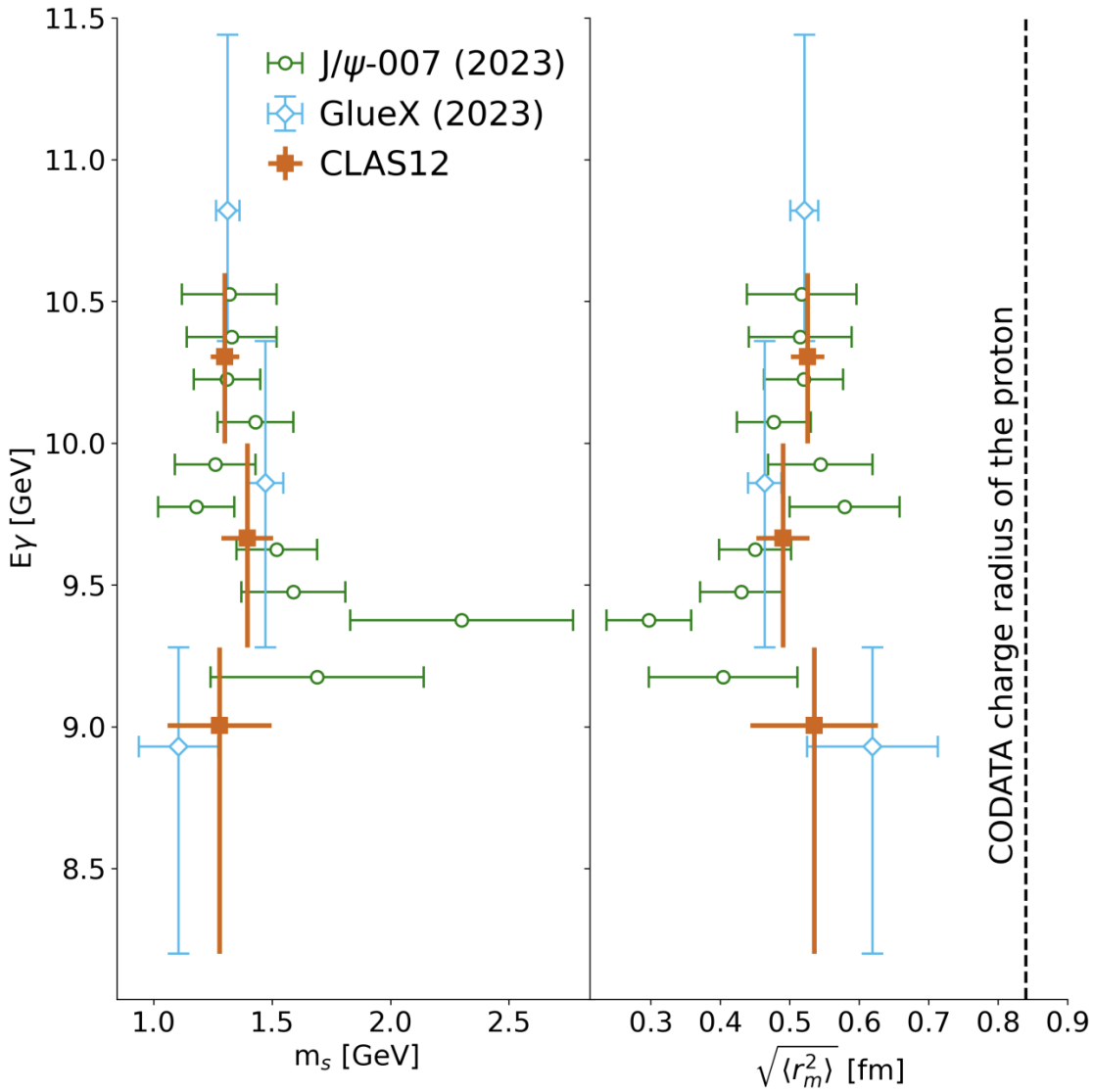

ExEx

Ex

Exs

Ex

- Ex